Neurobiology of Aging 69 (2018) 283–291

Contents lists available at ScienceDirect

Neurobiology of Aging

journal homepage: www.elsevier.com/locate/neuaging

# MicroRNA alterations in iPSC-derived dopaminergic neurons from Parkinson disease patients

Eduard Tolosa [a,b], Teresa Botta-Orfila [c,d], Xavier Morató [e,f], Carles Calatayud [g], Raquel Ferrer-Lorente [h,i], María-José Martí [a,b], Manel Fernández [a,b], Carles Gaig [a,b,j], Ángel Raya [h,i,k], Antonella Consiglio [g,l,m,**], Mario Ezquerra [a,b,*], Rubén Fernández-Santiago [a,b,*]

[a] Department of Neurology, Laboratory of Parkinson Disease and Other Neurodegenerative Movement Disorders, Hospital Clínic de Barcelona, Institut d'Investigacions Biomèdiques August Pi i Sunyer (IDIBAPS), University of Barcelona (UB), Barcelona, Spain
[b] Centro de Investigación Biomédica en Red de Enfermedades Neurodegenerativas (CIBERNED), Madrid, Spain
[c] Gene Function and Evolution Group, Centre for Genomic Regulation (CRG), Barcelona, Spain
[d] Universitat Pompeu Fabra (UPF), Barcelona, Spain
[e] Departament Patologia i Terapèutica Experimental, Unitat de Farmacologia, Facultat de Medicina, IDIBELL-Universitat de Barcelona, L'Hospitalet de Llobregat, Barcelona, Spain
[f] Institut de Neurociències, Universitat de Barcelona, Barcelona, Spain
[g] Department of Pathology and Experimental Therapeutics, Institute of Biomedicine of the University of Barcelona (IBUB), Bellvitge University Hospital-IDIBELL, Hospitalet de Llobregat, Barcelona, Spain
[h] Center of Regenerative Medicine in Barcelona (CMRB), Hospital Duran i Reynals, Hospitalet de Llobregat, Barcelona, Spain
[i] Centre for Networked Biomedical Research on Bioengineering, Biomaterials and Nanomedicine (CIBER-BBN), Madrid, Spain
[j] Department of Neurology, Multidisciplinary Sleep Unit, Hospital Clínic of Barcelona, Institut d'Investigacions Biomèdiques August Pi i Sunyer (IDIBAPS), University of Barcelona, Barcelona, Spain
[k] Institució Catalana de Recerca i Estudis Avançats (ICREA), Barcelona, Spain
[l] Department of Pathology and Experimental Therapeutics, Faculty of Medicine, IDIBELL- University of Barcelona, Barcelona, Spain
[m] Department of Molecular and Translational Medicine, University of Brescia and National Institute of Neuroscience, Brescia, Italy

ARTICLE INFO

*Article history:*
Received 27 March 2017
Received in revised form 23 May 2018
Accepted 24 May 2018
Available online 31 May 2018

*Keywords:*
Parkinson disease (PD)
microRNA (miRNA)
Leucine-rich repeat kinase 2 (LRRK2)
Dopaminergic neuron (DAn)
Transcription factor (TF)

ABSTRACT

MicroRNA (miRNA) misregulation in peripheral blood has been linked to Parkinson disease (PD) but its role in the disease progression remains elusive. We performed an explorative genome-wide study of miRNA expression levels in dopaminergic neurons (DAn) from PD patients generated by somatic cell reprogramming and induced pluripotent stem cells differentiation. We quantified expression levels of 377 miRNAs in DAn from 3 sporadic PD patients (sPD), 3 leucine-rich repeat kinase 2–associated PD patients (L2PD) (total 6 PD), and 4 healthy controls. We identified differential expression of 10 miRNA of which 5 were upregulated in PD (miR-9-5p, miR-135a-5p, miR-135b-5p, miR-449a, and miR-449b-5p) and 5 downregulated (miR-141–3p, miR-199a-5p, miR-299–5p, miR-518e-3p, and miR-519a-3p). Changes were similar in sPD and L2PD. Integrative analysis revealed significant correlations between miRNA/mRNA expression. Moreover, upregulation of miR-9-5p and miR-135b-5p was associated with downregulation of transcription factors related to the DNA hypermethylation of enhancer elements in PD DAn (*FOXA1* and *NR3C1*). In summary, miRNA changes are associated with monogenic L2PD and sPD and co-occur with epigenetic changes in DAn from PD patients.



## 1. Introduction

Parkinson disease (PD) is a progressive neurodegenerative disorder characterized by dopaminergic neural loss in the substantia nigra pars compacta (SNpc) and a related striatal dopamine deficit leading to the classical motor symptoms of bradykinesia, rigidity, and tremor (Lang and Lozano, 1998a,b). The vast majority of PD cases are sporadic (sPD) and believed to result from a complex interplay between genetic and environmental susceptibility factors of which aging is considered

* Corresponding authors at: Laboratory of Neurodegenerative Diseases, Faculty of Medicine (UB), Institut d'Investigacions Biomèdiques August Pi i Sunyer, (IDIBAPS), Hospital Clínic Universitari de Barcelona, University of Barcelona, Casanova 143, Floor 3B, CELLEX building, 08036, Barcelona, Italy. Tel.: +34 932 275 400 × 4814; fax: +34 932 275 783.
** Corresponding author at: Department of Pathology and Experimental Therapeutics, Stem Cells and Neurodegenerative Diseases Laboratory, Bellvitge University Hospital-IDIBELL, Hospitalet de Llobregat, Barcelona, 08908 Spain. Tel.: +34 934 039 842; fax: +34 93402155.
*E-mail addresses:* consiglio@ub.es (A. Consiglio), ezquerra@clinic.ub.es (M. Ezquerra), ruben.fernandez.santiago@gmail.com (R. Fernández-Santiago).

0197-4580/$ – see front matter © 2018 Elsevier Inc. All rights reserved.
https://doi.org/10.1016/j.neurobiolaging.2018.05.032

the most important known disease risk (Reeve et al., 2014). Yet around 5% encompass monogenic cases caused by pathogenic mutations segregating with disease in affected families (Gasser, 2009). Of these, missense mutations in the leucine-rich repeat kinase 2 (*LRRK2*) gene, most specially the toxic gain-of-function G2019S variant located in the kinase domain, are the most frequent cause of monogenic PD. Interestingly, *LRRK2* mutations have been identified not only in familial LRRK2-associated PD (L2PD) but also in many sPD cases suggesting a reduced penetrance which is determined by additional modifiers of their pathogenic expressivity (Fernández-Santiago et al., 2015b; Healy et al., 2008). Since L2PD can resemble clinically and neuropathologically sPD (Marras et al., 2016), this form is being widely used to model common sPD and to gain novel insights into the molecular alterations occurring in the disease.

MicroRNAs (miRNAs) are small noncoding regulatory RNAs controlling gene expression by the translational inhibition and degradation of their target mRNAs (Bartel, 2009). MiRNA alterations have been shown to contribute to the pathophysiology of neurodegenerative disorders (Abe and Bonini, 2013; Dimmeler and Nicotera, 2013). Mounting evidence has demonstrated differential miRNA expression changes in peripheral tissues from PD patients such as whole blood (Alieva et al., 2015; Margis et al., 2011; Martins et al., 2011; Serafin et al., 2015; Soreq et al., 2013), plasma (Cardo et al., 2014; Khoo et al., 2012), and serum (Botta-Orfila et al., 2012; Vallelunga et al., 2014) even at PD prodromal stages before clinical manifestation of the motor symptoms (Fernandez-Santiago et al., 2015c). These studies have suggested a potential role of miRNAs as candidate biomarkers for the diagnosis and prognosis of PD (Danborg et al., 2014). However, miRNA studies in the central nervous system have been hindered by the inaccessibility to dopaminergic neurons (DAns) from live patients. Yet reports in postmortem PD brain tissue have also shown that miRNA deregulation of at least some specific miRNAs also occurs at advanced stages of disease (Fuchs et al., 2009; Kim et al., 2007). Because of the limiting cell inaccessibility, the miRNA expression profile of DAn from PD patients at more initial stages of the neurodegenerative process remains unknown until date.

Upon cell reprogramming of skin fibroblasts from patients with sPD and L2PD into induced pluripotent stem cells (iPSC) and their differentiation into DAns, we have previously generated and characterized a patient-derived disease-specific DAn model of PD (Fernandez-Santiago et al., 2015a; Sanchez-Danes et al., 2012b). In these iPSC-derived DAn cells, we have reported large epigenomic changes consisting in an aberrant DNA methylation profile which was associated with both sPD and L2PD (Fernandez-Santiago et al., 2015a). These epigenomic changes detected in PD iPSC-derived DAn antedated disease-specific phenotypes emerging on long-term culture, which included reduced axonal outgrowth, impaired autophagic vacuole clearance, and accumulation of alpha-synuclein (Sanchez-Danes et al., 2012b). The same patient DAn cell lines from these 2 previous studies were used here to further perform an unbiased genome-wide miRNA expression study interrogating the expression levels of 377 miRNAs in 3 sPD patients, 3 L2PD patients, and 4 healthy controls. More specifically, here we have investigated whether specific miRNA expression modifications occur in iPSC-derived DAn from sPD as well as familial L2PD, and concurrently we have also explored a potential functional relation between miRNA and global gene expression changes observed in our model.

## 2. Material and methods

### 2.1. Study approval

The study conformed to the principles of the Declaration of Helsinki and the Belmont Report. All participants gave written informed consent, and the study was approved by the Commission on Guarantees for Donation and Use of Human Tissues and Cells of the Instituto de Salud Carlos III and the ethics committee from the Hospital Clínic de Barcelona. Personal data were anonymized and subject samples were codified to preserve confidentiality.

### 2.2. Subjects and generation of iPSC-derived DAn cell lines

Studied individuals included 3 patients with sPD reporting no family history of disease, who were negative in the *LRRK2* mutational screening, 3 patients with familial L2PD, who carried the *LRRK2* G2019S mutation, and 4 genetically unrelated healthy controls without familial history of neurological disease. Clinical details from the patients and controls are summarized in Table 1. Skin biopsies of 3 mm of diameter were performed in the alar surface of the forearm of subjects and primary cultures of somatic skin cells (keratinocytes and fibroblasts) were established. Cell reprogramming of somatic cells into iPSC was done based on the retroviral delivery of a cocktail of 3 reprogramming factors including *OCT4*, *KLF4*, and *SOX2*. Differentiation of iPSCs into DAn was carried out by the lentiviral delivery of the A9-subtype DAn pattering factor *LMX1A*, which enriches by 4-fold the yield of DAn, and co-culture with mouse PA6 feeding cells. Reprogramming and differentiation protocol (Sanchez-Danes et al., 2012a) and cell line characterization of the DAn used in the present study have been previously described elsewhere (Fernandez-Santiago et al., 2015a; Sanchez-Danes et al., 2012b). After 30-days of differentiation, resulting iPSC-derived DAns were subjected to miRNA expression profiling and also to the genome-wide gene expression and DNA methylation analyses previously published (Fernandez-Santiago et al., 2015a).

### 2.3. miRNA isolation

Total RNA containing enriched small RNAs (18 nucleotides upward) was isolated from 1 million cells using the miRNeasy Kit (Qiagen) according to manufacturer instructions and resuspended in 30 μL of RNase-free water. Total RNA concentration and quality were determined in a Nanodrop 1000 spectrophotometer (Thermo Fisher Scientific). Average RNA yield using this method was of 10 μg at a mean concentration of 300 ng/μL per sample.

### 2.4. miRNA expression analysis

Retro-transcription of 400 ng of RNA samples enriched in miRNA into cDNA was performed using the Megaplex RT Primer Pools - Human Pool A (Applied Biosystems, product datasheet: https://tools.thermofisher.com/content/sfs/manuals/4399721c.pdf) in a PTC-200 thermocycler (MJ Research). We mixed 6 μL of each cDNA product with a total of 394 μL of nuclease-free water and 400 μL of TaqMan Master Mix and loaded 100 μL of the quantitative real-time PCR (qPCR) reaction mix in each port of the TaqMan Array Human MicroRNA A Cards v2.0 (Applied Biosystems, product datasheet: https://tools.thermofisher.com/content/sfs/manuals/cms_042326.pdf), also known as TaqMan Low Density Array. Samples were centrifuged 2 times at 110 g during 1 minute and miRNA amplification was performed in a Viia7 1.0 Real-Time PCR system (Applied Biosystems). Raw data were filtered out using the Expression Suite v1.0 software (Applied Biosystems). Out of the 377 miRNAs included in the array, we considered for subsequent analyses only the quantification cycle values from miRNAs expressed below 35 cycles in at least 50% of the samples, resulting in a total of 240 miRNAs. Relative quantification of miRNA expression levels was done using the $-\Delta Ct$ algorithm in the DataAssist software v3.0 (Applied Biosystems). As endogenous normalizing controls, we selected miRNAs showing the best normalization score (MammU6,

**Table 1**
Clinical details of PD patients and iPSC-derived DAn cell lines characterized by genome-wide miRNA expression analysis

| Cell line code | Code previous study[c] | Subject type | *LRRK2* mutation | Family history of PD | Gender | Age at donation | Age at onset | Initial symptoms | L-DOPA response | Selected iPSC clone | Cell ratio TUJ1$^+$/DAPI$^+$ (neurons)[a] | Cell ratio TH$^+$/TUJ1$^+$ (DA neurons)[b] |
|---|---|---|---|---|---|---|---|---|---|---|---|---|
| C-01 | SP-15 | Control | No | No | Female | 47 | - | - | - | 15–2 | 34.7 | 45.0 |
| C-02 | SP-11 | Control | No | No | Female | 48 | - | - | - | 11–1 | 40.0 | 59.9 |
| C-03 | SP-09 | Control | No | No | Male | 66 | - | - | - | 9–4 | 52.2 | 55.5 |
| C-04 | SP-17 | Control | No | No | Male | 52 | - | - | - | 17–2 | 54.0 | 65.8 |
| PD-01 | SP-13 | L2PD | G2019S | Yes | Female | 68 | 57 | T | Good | 13–4 | 47.0 | 65.2 |
| PD-04 | SP-16 | sPD | No | No | Female | 51 | 48 | B | N/A | 16–2 | 32.1 | 55.2 |
| PD-05 | SP-06 | L2PD | G2019S | Yes | Male | 44 | 33 | T | Good | 6–2 | 40.9 | 61.9 |
| PD-07 | SP-12 | L2PD | G2019S | Yes | Female | 63 | 49 | T | Good | 12–3 | 42.7 | 60.0 |
| PD-09 | SP-01 | sPD | No | No | Female | 63 | 58 | T and B | N/A | 1–1 | 32.2 | 44.9 |
| PD-10 | SP-08 | sPD | No | No | Female | 66 | 60 | T | Good | 8–1 | 41.6 | 67.1 |

Key: B, bradykinesia; D, foot dystonia; DAn, dopaminergic neuron; iPSC, induced pluripotent stem cell; L2PD, LRRK2-associated PD; miRNA, microRNA; N/A, not assessed; PD, Parkinson disease; sPD, sporadic PD; T, tremor.

[a] Ratio of neurons/total cells, calculated by immunofluorescence as the ratio of TUJ1 (neuron-specific class III b-Tubulin)-positive cells/DAPI-positive cells.

[b] Ratio of iPSC-derived DAn/total neurons, calculated by immunofluorescence as the ratio of TH (tyrosine hydroxylase)-positive cells/TUJ1 positive cells.

[c] Sanchez-Danes, A. et al., 2012b. Disease-specific phenotypes in dopamine neurons from human iPS-based models of genetic and sporadic Parkinson's disease. EMBO Mol Med. 4(5):380–395. Fernández-Santiago, R. et al., 2015a. Aberrant epigenome in iPSC-derived dopaminergic neurons from Parkinson's disease patients. EMBO Mol Med. 7, 1529–1546.

RNU48, miR-26a, miR-484, miR-744, and miR-26b) according to a method that has been previously described (Vandesompele et al., 2002).

### 2.5. Identification of differentially expressed miRNAs

We performed pairwise comparisons between the groups of study—sPD, L2PD, total PD, and controls—using a 2-tailed Student *t*-test. For each miRNA, we calculated the difference between the expression levels in the 2 groups under comparison as relative quantity values (equivalent to fold-change values). We set the statistical significance threshold for differential miRNA expression at *P* below 0.05 after multiple-testing adjustment of *p* values by using the false discovery rate correction (Benjamini and Hochberg, 1995) as implemented in the DataAssist v3.0 software. The number of tests was of 240 corresponding to the number of miRNA expressed in all iPSC-derived DAn samples (quantification cycle below 35 cycles) (Table 2). We used the DataAssist v3.0 pipeline for the hierarchical clustering analysis of differentially expressed miRNAs (DEmiR) using the average linkage as clustering algorithm and the Pearson correlation coefficient as distance measure (Fig. 1).

### 2.6. Quantitative real-time PCR validation

As a technical validation, by qPCR using individual TaqMan miRNA assays, we assessed the expression of the top 5 most significant DEmiR detected in the array (miR-135a-5p, miR-135b-5p, miR-449a, miR-449b-5p, and miR-199a-5p) in the same miRNA samples screened in the array (6 PD vs. 4 controls) (Supplemental Table 1). Alternatively, we also performed a total RNA extraction from these samples (RNeasy Kit, Quiagen, # 74104). We retro-transcribed a total of 2 μg of total RNA into cDNA using a high-capacity cDNA reverse transcription kit (Thermo Fisher Scientific, #4368814) according to manufacturer instructions in a PTC-200 thermocycler (MJ Research) and diluted cDNA products 1/10 into RNase-free water. We performed qPCR using commercially available TaqMan MicroRNA assays (Applied Biosystems) for the tested DEmiR hsa-miR-135a-5p (#000460), hsa-miR-135b-5p (#002261), hsa-miR-449a (#001030), hsa-miR-449b-5p (#001608), and hsa-miR-199a-5p (#000498), and also for the house-keeping miRNAs hsa-miR-744 (#002324),and RNU48 (#001006). We selected the latter among miRNA showing the most stable expression across all samples as analyzed by using using DataAssist v3.0 algorithm (Thermo Fisher Scientific) as described previously (Vandesompele et al., 2002). We mixed 4 μl of each sample with the appropriate volume of nuclease-free water and TaqMan Gene Expression Master Mix (Applied Biosystems, # 4369016) and quantified miRNA expression in a StepOnePlus Real-Time PCR system (Thermo Fisher Scientific). We computed raw data values for miRNA quantification using the DataAssist software 3.0. Using this method and as a biological validation, we also assessed the expression of these top 5 most significant DEmiR in total RNA samples (RNeasy Kit, Quiagen, # 74104) isolated from iPSC-derived DAn samples of 3 additional PD patients (Supplemental Table 2), which were compared to the 4 healthy controls previously described.

### 2.7. Biological enrichment analysis of genes targeted by miRNAs

We explored the biological enrichment of genes targeted by the identified DEmiR using the software DIANA-miRPath v3.0

**Table 2**
DEmiR associated with PD ordered by statistical significance

| Differentially expressed microRNA (DEmiR) | Assay commercial code (ABI) | Mean $2^{-\Delta Ct}$ expression levels ±S.D. in PD | Mean $2^{-\Delta Ct}$ expression levels ±S.D. in controls | Fold change | Expression change | *p*-value | Multiple testing adj. *p*-value |
|---|---|---|---|---|---|---|---|
| hsa-miR-135a-5p | 4,373,140 | 0.300 ± 0.140 | 0.011 ± 0.005 | 26.78 | Upregulated | 0.000017 | 0.004 |
| hsa-miR-135b-5p | 4,395,372 | 0.313 ± 0.060 | 0.059 ± 0.013 | 5.26 | Upregulated | 0.0001 | 0.006 |
| hsa-miR-449a | 4,373,207 | 0.380 ± 0.250 | 0.007 ± 0.005 | 51.76 | Upregulated | 0.0001 | 0.007 |
| hsa-miR-449b-5p | 4,381,011 | 0.150 ± 0.095 | 0.003 ± 0.002 | 40.97 | Upregulated | 0.0001 | 0.007 |
| hsa-miR-199a-5p | 4,373,272 | 0.329 ± 0.145 | 0.822 ± 0.414 | −3.33 | Downregulated | 0.0008 | 0.035 |
| hsa-miR-299−5p | 4,373,188 | 0.001 ± 5.5E-5 | 0.003 ± 0.001 | −3.33 | Downregulated | 0.0009 | 0.035 |
| hsa-miR-518e-3p | 4,395,506 | 0.0026 ± 0.001 | 0.067 ± 0.060 | −24.39 | Downregulated | 0.0011 | 0.035 |
| hsa-miR-9-5p | 4,373,285 | 2.280 ± 2.130 | 0.018 ± 0.015 | 133.06 | Upregulated | 0.0012 | 0.035 |
| hsa-miR-141−3p | 4,373,137 | 0.009 ± 0.004 | 0.026 ± 0.007 | −2.94 | Downregulated | 0.0014 | 0.035 |
| hsa-miR-519a-3p | 4,395,526 | 0.003 ± 0.0009 | 0.054 ± 0.042 | −17.00 | Downregulated | 0.0016 | 0.035 |

Key: PD, Parkinson disease; S.D., standard deviation.

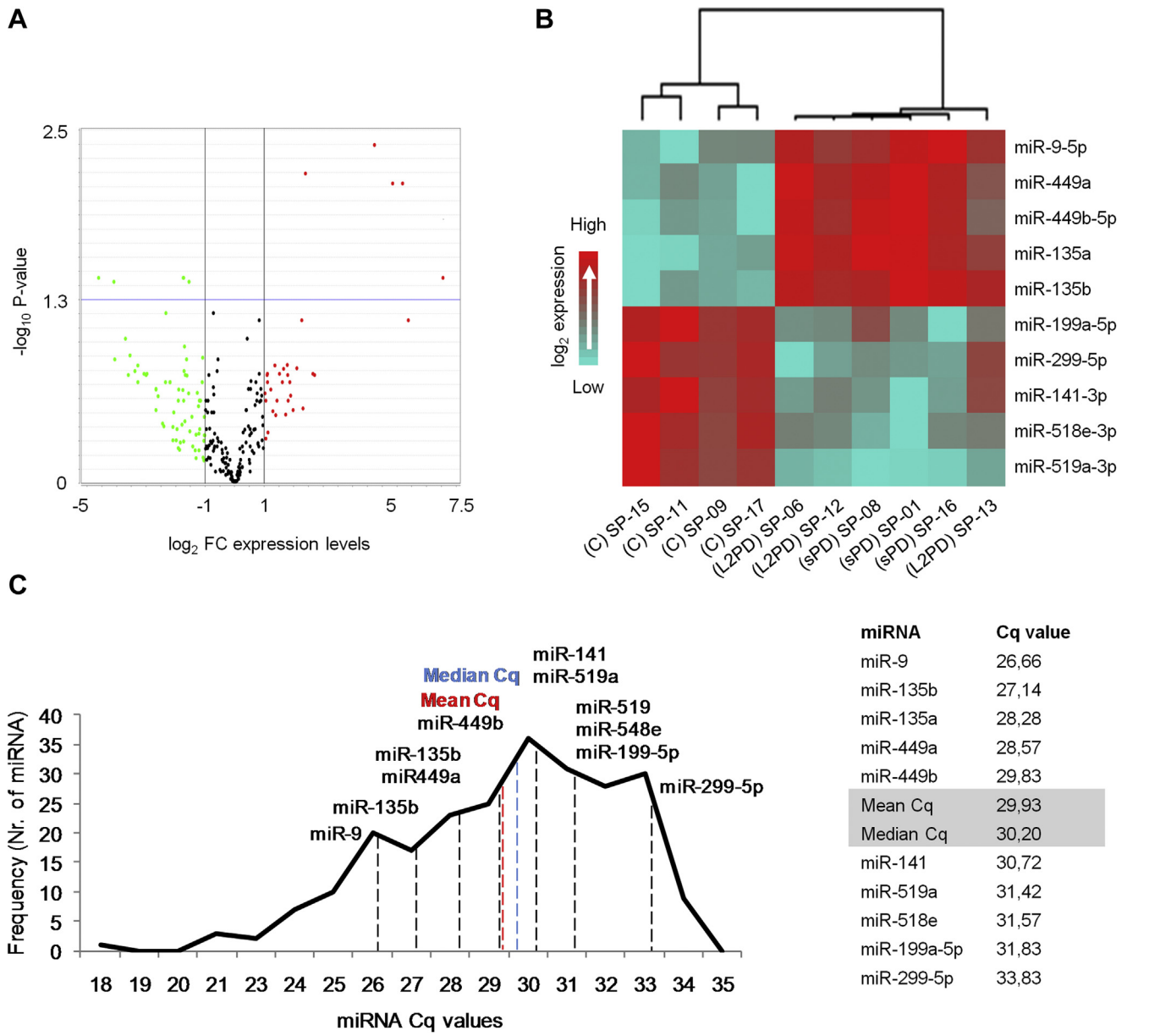


**Fig. 1.** Identification of DEmiR in iPSC-derived DAn from PD patients. (A) Volcano plot showing upregulated DEmiR in upper right and downregulated DEmiR in upper left quadrants. Horizontal axis represents relative miRNA expression levels between PD and controls, whereas vertical axis represents *p*-value. (B) Heatmap showing the 10 DEmiR associated with PD and density color code for miRNA expression levels showing discrimination between PD either sPD or L2PD, and healthy controls. (C) Representation of miRNA Cq values showing the Cq values of the PD-associated DEmiR in relation to the mean (Cq = 30.20) and to the median (Cq = 29.93) observed for all miRNAs screened in the array. Abbreviations: Cq, quantification cycle; DAn, dopaminergic neuron; DEmiR, differentially expressed miRNA; iPSC, induced pluripotent stem cell; L2PD, LRRK2-associated PD; miRNA, microRNA; PD, Parkinson disease; sPD, sporadic PD.

(Vlachos et al., 2015b). This tool identifies miRNA/target gene interactions (http://www.microrna.gr/miRPathv3) and is based on more than half a million of experimentally reported interactions and the DIANA-TarBase v7 algorithm (Vlachos et al., 2015a). Subsequently, we performed a miRNA-target gene biological enrichment analysis and identified affected canonical pathways using the DAVID extension (https://david.ncifcrf.gov) of DIANA-miRPath v3.0. To this end, we used both the union analysis mode including the summatory effect of independent miRNAs and also the more conservative gene intersection mode considering only genes simultaneously targeted by at least 3 different miRNAs (Supplemental Table 3).

### 2.8. Association of miRNA and gene expression changes

We overlapped DEmiR expression data with global gene expression data from 437 differentially expressed genes (DEGs) identified in the same DAn cell lines from PD patients by a genome-wide transcriptomic analysis covering 96% of the transcriptome (Fernandez-Santiago et al., 2015a). These DEG data are deposited in the Gene Expression Omnibus under accession number GSE51922. For identifying specific DEmiR/DEG pairs, we used the MAGIA software (Sales et al., 2010) (http://genc_omp_bio_unipd_it/magia/start/). The MAGIA pipeline detects miRNA/mRNA significant correlations based on both predictive and experimentally observed

correlations. We considered only DEmiR/DEG interactions identified simultaneously by 3 independent algorithms including miRanda (stringency score 20), PITA (stringency score 300), and Targetscan, with a Spearman correlation coefficient (r) above |0.60|, and with a multiple testing adjusted *P* below 0.05 (Supplemental Table 4).

### 2.9. Functional network analysis of miRNA and gene expression changes

We used the DEmiR and DEG interaction data described above to build interaction networks by using the MAGIA software. For network visualization, we used the Cytoscape software (www.cytoscape.org) (Shannon et al., 2003). In the DEmiR/DEG network, yellow nodes represent DEmiRs, whereas white nodes represent DEGs, the sizes of nodes are proportional to the number of direct interactions, and the thicknesses of edges are proportional to the degree of correlation (Fig. 2). We also performed a biological enrichment analysis of identified DEmiR/DEG pairs by using the DAVID software (https://david.ncifcrf.gov) (Table 3).

## 3. Results

We performed a comprehensive genome-wide analysis of miRNA expression levels in iPSC-derived DAn from PD patients and controls. Out of the 377 screened miRNAs, a total of 240 miRNAs showed detectable and quantifiable expression levels in our samples. Before statistical analysis, unsupervised hierarchical clustering of expression values from these 240 miRNAs showed expression profiles which mostly differentiated between PD patients (L2PD and sPD) and healthy controls suggesting overall miRNA expression differences between these 2 groups (Supplemental Fig. 1). We then first compared the sPD and L2PD groups under a multiple testing adjusted *P* below 0.05 and found no DEmiR in between these 2 forms of disease indicating similar miRNA expression profiles. Using the same conditions of above, we further identified 10 DEmiR in the PD group as a whole as compared to controls (Table 2). Of these, 5 DEmiR were significantly upregulated in PD (miR-miR-9-5p, 135a-5p, miR-135b-5p, miR-449a, and miR-449b-5p), whereas 5 were downregulated (miR-141−3p, miR-199a-5p, miR-299−5p, miR-518e-3p, and miR-519a-3p) (Fig. 1). Collectively, these data indicate that DAn from PD patients show alterations in miRNA expression compared to healthy controls. They also indicate that sPD and L2PD share similar miRNA expression changes.

We further performed a qPCR validation using individual TaqMan miRNA assays for the top 5 most significant DEmiR detected in the arrays (miR-135a-5p, miR-135b-5p, miR-449a, miR-449b-5p, and miR-199a-5p). We observed similar fold-change values by qPCR and by array for miR-135a-5p (23.55 vs. 26.78), miR-135b-5p (2.85 vs. 5.26), miR-449a (37.23 vs. 51.76), miR-449b-5p (32.63 vs. 40.97), and miR-199a-5p (−2.56 vs. −3.33), respectively. Overall, we found a high degree of correlation between both experiments (Pearson correlation coefficient r = 0.9929 and r2 = 0.9859), thus validating the miRNA findings detected in the array. In the biological validation using 3 additional PD patients, either alone or pooled with the 6 original PD subjects, and compared to the controls, we found similar miRNA changes as those observed with the array (Supplemental Tables 1 and 2).

We next explored the molecular functions regulated by the identified DEmiR by performing an in silico biological enrichment

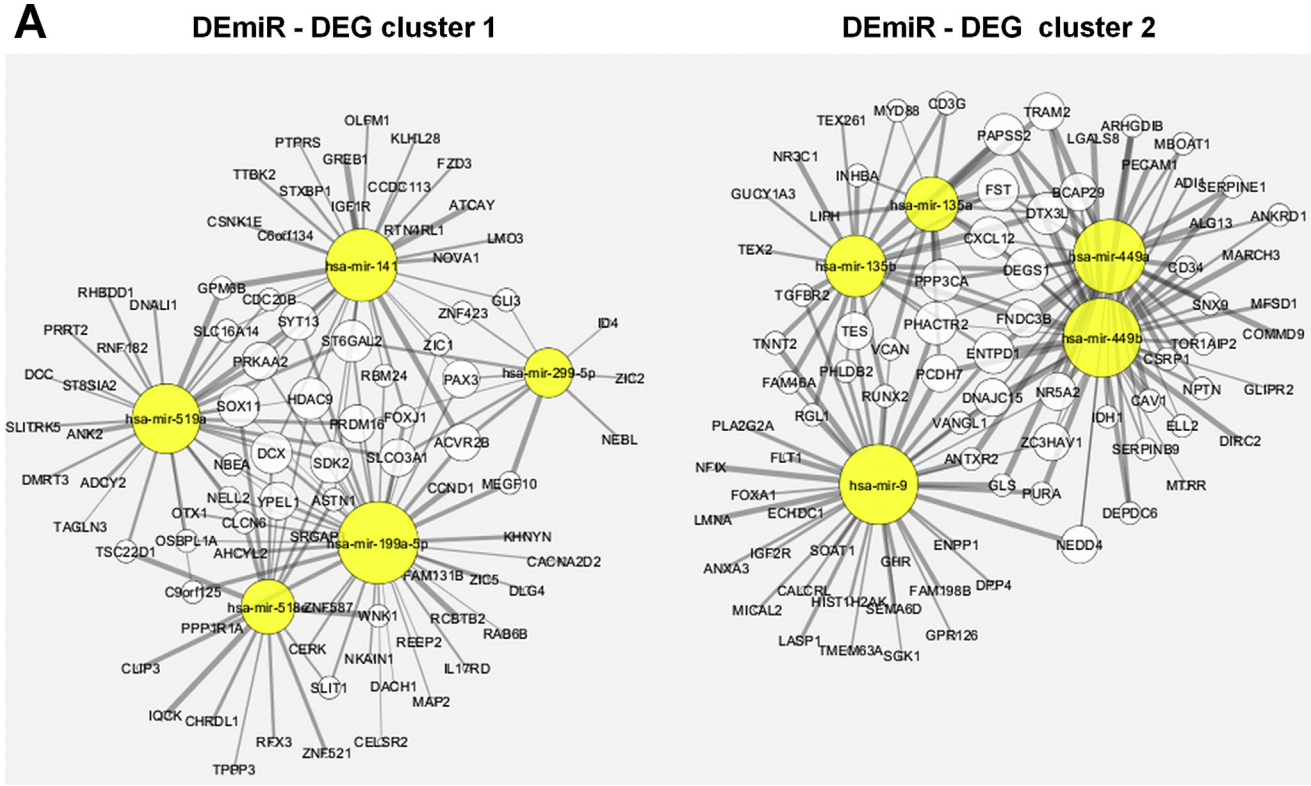


**Fig. 2.** Interaction network of DEmiR and DEG identified in iPSC-derived DAn from PD patients showing 2 interaction clusters. Cluster 1 encompasses PD downregulated DEmiR, and their respective interacting DEGs, whereas cluster 2 involves PD upregulated DEmiR. DEmiR are represented in yellow and DEG in white. The sizes of the DEmiR-DEG nodes are proportional to the number of direct DEmiR-DEG interactions, and thicknesses of edges from DEmiR to DEG are proportional to the degree of correlation. Abbreviations: DAn, dopaminergic neuron; DEG, differentially expressed gene; DEmiR, differentially expressed miRNA; iPSC, induced pluripotent stem cell; miRNA, microRNA; PD, Parkinson disease. (For interpretation of the references to color in this figure legend, the reader is referred to the Web version of this article.)

**Table 3**
Biological enrichment analysis of DEmiR/DEG pairs from interaction clusters 1 and 2 identified in PD

| Gene ontology (GO) term | Nr. of genes | Total of genes | *p* value | Benjamini adj. *p* value |
|---|---|---|---|---|
| Cluster 1 terms (downregulated DEmiR, upregulated DEG) | | | | |
| GO:0030182 ~ neuron differentiation | 13 | 63 | 5.68E−07 | 4.59E−04 |
| GO:0048858 ~ cell projection morphogenesis | 10 | 63 | 1.59E−06 | 6.43E−04 |
| GO:0032990 ~ cell part morphogenesis | 10 | 63 | 2.29E−06 | 6.16E−04 |
| GO:0031175 ~ neuron projection development | 10 | 63 | 2.29E−06 | 6.16E−04 |
| GO:0048667 ~ cell morphogenesis involved in neuron differentiation | 9 | 63 | 4.69E−06 | 9.47E−04 |
| GO:0048812 ~ neuron projection morphogenesis | 9 | 63 | 5.40E−06 | 8.72E−04 |
| GO:0030030 ~ cell projection organization | 11 | 63 | 5.99E−06 | 8.06E−04 |
| GO:0000904 ~ cell morphogenesis involved in differentiation | 9 | 63 | 1.46E−05 | 0.0017 |
| GO:0048666 ~ neuron development | 10 | 63 | 2.21E−05 | 0.0022 |
| GO:0007409 ~ axonogenesis | 8 | 63 | 2.73E−05 | 0.0025 |
| GO:0000902 ~ cell morphogenesis | 10 | 63 | 3.24E−05 | 0.0026 |
| GO:0032989 ~ cellular component morphogenesis | 10 | 63 | 7.55E−05 | 0.0055 |
| GO:0060562 ~ epithelial tube morphogenesis | 5 | 63 | 2.47E−04 | 0.0165 |
| GO:0021915 ~ neural tube development | 5 | 63 | 2.62E−04 | 0.0161 |
| GO:0001843 ~ neural tube closure | 4 | 63 | 3.41E−04 | 0.0195 |
| GO:0060606 ~ tube closure | 4 | 63 | 3.41E−04 | 0.0195 |
| GO:0014020 ~ primary neural tube formation | 4 | 63 | 4.53E−04 | 0.0241 |
| GO:0048598 ~ embryonic morphogenesis | 8 | 63 | 4.89E−04 | 0.0244 |
| GO:0001841 ~ neural tube formation | 4 | 63 | 8.03E−04 | 0.0374 |
| Cluster 2 terms (upregulated DEmiR, downregulated DEG) | | | | |
| GO:0044057 ~ regulation of system process | 9 | 64 | 8.80E−05 | 0.0950 |
| GO:0006790 ~ sulfur metabolic process | 6 | 64 | 1.93E−04 | 0.1038 |
| GO:0051094 ~ positive regulation of developmental process | 8 | 64 | 2.97E−04 | 0.1063 |
| GO:0045597 ~ positive regulation of cell differentiation | 7 | 64 | 6.69E−04 | 0.1730 |
| GO:0032101 ~ regulation of response to external stimulus | 6 | 64 | 8.55E−04 | 0.1764 |
| GO:0006898 ~ receptor-mediated endocytosis | 4 | 64 | 0.0019 | 0.3035 |
| GO:0019915 ~ lipid storage | 3 | 64 | 0.0031 | 0.3968 |
| GO:0048754 ~ branching morphogenesis of a tube | 4 | 64 | 0.0034 | 0.3852 |
| GO:0006897 ~ endocytosis | 6 | 64 | 0.0036 | 0.3617 |
| GO:0010324 ~ membrane invagination | 6 | 64 | 0.0036 | 0.3617 |
| GO:0001569 ~ patterning of blood vessels | 3 | 64 | 0.0042 | 0.3822 |
| GO:0006937 ~ regulation of muscle contraction | 4 | 64 | 0.0046 | 0.3765 |
| GO:0001763 ~ morphogenesis of a branching structure | 4 | 64 | 0.0049 | 0.3735 |
| GO:0051241 ~ negative regulation of multicellular organismal process | 5 | 64 | 0.0071 | 0.4641 |
| GO:0016044 ~ membrane organization | 7 | 64 | 0.0084 | 0.4970 |
| GO:0048661 ~ positive regulation of smooth muscle cell proliferation | 3 | 64 | 0.0091 | 0.4993 |
| GO:0048878 ~ chemical homeostasis | 8 | 64 | 0.0095 | 0.4905 |
| GO:0042127 ~ regulation of cell proliferation | 10 | 64 | 0.0102 | 0.4970 |
| GO:0006940 ~ regulation of smooth muscle contraction | 3 | 64 | 0.0135 | 0.5748 |

Key: DEmiR, differentially expressed miRNA; DEG, differentially expressed gene; GO, gene ontology; PD, Parkinson disease.

analysis of their predicted target genes. To this end, we overlapped the PD-associated DEmiR data with experimentally validated miRNA/target-gene interaction data, which are publically available at the DIANA-miRPath database (Vlachos et al., 2015b). We used the union analysis mode that considers the summatory effect of independent DEmiR and also the more conservative intersection mode considering only genes simultaneously targeted at least by 3 different DEmiRs. Significantly enriched gene ontology biological processes and Kyoto Encyclopedia of Genes and Genomes pathways included canonical pathways involved in cancer including melanoma, extracellular matrix, cytoskeleton dynamics, and PI3K kinase/Akt cell signaling (Supplemental Table 3). These results suggest an effect of the PD-associated miRNA expression changes on the cytoskeleton, axonal transport, cell adhesion, and cell survival in PD.

We then analyzed the relationship between PD differential miRNA expression and previously observed gene expression changes from the same DAn lines (Fernandez-Santiago et al., 2015a). We found a significant association of 590 DEmiR/DEG pairs under a Spearman correlation coefficient (r) above |0.6| and a multiple testing adjusted *P* below 0.05 (See Material and Methods). Of these, 285 associations were inverse and affected to a total of 167 different genes, whereas 305 were positive (Supplemental Table 4). On the other hand, apart from expected direct negative associations mediated by the direct binding of DEmiR to specific motifs at the 3′-UTR of regulated genes, positive associations have also been previously reported in the literature (Ritchie et al., 2009). These positive associations are thought to operate by indirect interactions through the binding and degradation of DEmiR to intermediate molecules such as transcription inhibitors operating between the DEmiR and the controlled genes, thus leading to their upregulation (Ritchie et al., 2009). Overall, our findings suggest that miRNA expression changes occurring in PD play a role in regulating gene expression, both inversely and positively.

We further performed a functional network analysis of DEmiR and DEG correlating pairs. We focused only on inverse DEmiR/DEG associations to specifically analyze classical direct downregulation effects of miRNA on RNAs. We found 2 independent clusters (Fig. 2). Cluster 1 encompassed the PD downregulated DEmiRs miR-141−3p, miR-199a-5p, miR-299−5p, miR-518e-3p, and miR-519a-3p, and associated DEGs, which, interestingly, were largely involved in specific neural functions such as neuron differentiation, neural projection development, or axonogenesis among others (Table 3). In addition, cluster 2 included the PD upregulated DEmiRs miR-135a, miR-135b, miR-449a, miR-449b-5p, miR-9-5p, and associated DEGs, which were related to diverse homeostatic functions such as regulation of response to external stimulus, endocytosis, or metabolic processes. Previously, we have shown that PD upregulated DEGs were overall involved in neural functions, whereas downregulated DEGs in different homeostasis processes (Fernandez-Santiago et al., 2015a). Thus, our miRNA data here complement previous expression data in PD DAn by adding a new

layer of molecular information which collectively suggest that the downregulation of specific miRNA is related to enhancement of specific neural functions, whereas the upregulation of other miRNA is associated with the downregulation of basic homeostasis in PD.

We then dissected specific DEmiR/DEG inversely associated pairs. We found that the PD upregulation of miR-9-5p was associated with the expression downregulation of the transcription factor (TF) *FOXA1* ($r = -0.87$, adj. $p = 0.0052$), whereas, in the same direction, the upregulation of miR-135b-5p was related to the downregulation of the TF *NR3C1* ($r = -0.71$, adj. $p = 0.0308$) (Supplemental Table 4). We previously showed that the gene expression deficit of *FOXA1* and *NR3C1*, among other TFs, was related to the DNA hypermethylation of enhancer elements in iPSC-derived DAn from PD patients (Fernandez-Santiago et al., 2015a). Contrariwise, we also found that the downregulation of miR-199a-5p was associated with the gene expression upregulation of *ZIC1* ($r = -0.93$, adj. $p = 0.0012$), *NELL2* ($r = -0.90$, adj. $p = 0.0024$), and *OTX1* ($r = -0.87$, adj. $p = 0.0052$), whereas, in the same direction, the downregulation of miR-519a-3p was related to the upregulation of *DCC* ($r = -0.90$, adj. $p = 0.0062$). Previously, we reported that *ZIC1*, *NELL2*, *OTX1*, and *DCC* among others are top DEGs involved in neural functions showing differential gene expression upregulation in PD (top-20 list of 437 DEGs) (Fernandez-Santiago et al., 2015a). Altogether, these data suggest that the specific miRNA expression changes in PD could be related to the aberrant DNA methylation mediated by the deficit of key TFs *FOXA1* and *NR3C1* and also to specific gene expression changes observed in our DAn model.

## 4. Discussion

We report the first explorative genome-wide study of miRNA expression levels in iPSC-derived DAn from PD patients, with either sPD or monogenic L2PD. After multiple-testing adjustment, we identified differential expression of 10 miRNA in PD patients as compared to controls of which 5 DEmiR were upregulated in PD (miR-miR-9-5p, 135a-5p, miR-135b-5p, miR-449a, and miR-449b-5p), whereas 5 were downregulated (miR-141−3p, miR-199a-5p, miR-299−5p, miR-518e-3p, and miR-519a-3p).

Among PD upregulated DEmiR, changes in miR-9-5p, miR-135a-5p, and miR-135b-5p expression were previously associated with PD in studies using samples from PD patients, whereas miR-449a and miR-449b-5p have also been linked to disease in other studies using PD models. miRNA miR-9-5p was found to be upregulated in peripheral blood from PD patients (Alieva et al., 2015). Moreover, upregulation of miR-9 was associated with downregulated expression of glial cell line–derived neurotrophic factor, a key neurotrophin that increases the number of adult DAn in the SNpc and promotes survival of DAn both in vivo and in vitro (Kumar et al., 2015). miRNA miR-135a-5p was recently identified as upregulated DEmiR in a study using laser micro-dissected midbrain DAn from postmortem SNpc brain of 8 idiopathic PD patients and 8 controls and the same miRNA array employed in the present study (Briggs et al., 2015). Interestingly, miR-135a-5p is involved in delimiting the dorso-ventral extent and allocation of DAn progenitors by targeting *LMX1B* and other genes of the Wnt signaling pathway during midbrain development (Anderegg et al., 2013). Also, miR-135a-5p has been reported to be compensatorily protective in adult DAn of a 1-methyl-4-phenyl-1,2,3,6-tetrahydropyridine subacute mouse model of PD (Liu et al., 2016). In addition, expression levels of the functionally closely related miR-135b-5p (Anderegg et al., 2013) were found to be deregulated in SNpc from PD patients (Cardo et al., 2014) and also in cerebrospinal fluid (CSF) from Alzheimer's disease patients (Liu et al., 2014). Finally, miR-449a and miR-449b are involved in normal brain development and microtubule dynamics (Wu et al., 2014) and have been predicted to target a-synuclein, the major aggregating protein found in Lewy bodies from PD patients (Heman-Ackah et al., 2013). In addition, another study has shown deregulation of miR-9 and miR-449b in putamen and also in CSF from PD patients (Hesse and Arenz, 2014).

Regarding DEmiR downregulated in PD, reduced expression of miR-141-3p, miR-199a-5p, and miR-299-5p was recently reported in biological samples from PD patients, whereas miR-518e-3p and miR-519a-3p deregulation has not been previously related to PD. Thus, miRNA miR-141 expression levels were significantly diminished in serum from PD patients at early Hoehn and Yahr motor stages I and II (Dong et al., 2016). Moreover, a recent study applying a systems biology approach has identified miR-141-3p as hub miRNA in a TF-miRNA-mRNA regulatory network involved in PD and postulated this miRNA as potential novel biomarker and therapeutic target in PD (Chatterjee et al., 2014). In addition, miRNA miR-199a-5p has been shown to be downregulated in peripheral blood mononuclear cells from PD patients (Martins et al., 2011) and this miRNA was also predicted to target a-synuclein (Heman-Ackah et al., 2013). Furthermore, expression levels of miR-299-5p have also been found to be downregulated in SNpc from PD patients (Cardo et al., 2014). Finally, miR-518e-3p and miR-519a-3p have shown upregulated expression in specific types of cancer (Flor et al., 2016; Wei et al., 2016) but their potential involvement in neurodegenerative diseases has not been previously reported.

We showed that genes targeted by the identified DEmiR were involved in regulating cytoskeleton dynamics, axonal transport, cell adhesion and cell survival, comprising canonical pathways previously shown to be altered in PD (Edwards et al., 2011; Grunblatt et al., 2004; Mandel et al., 2005; Mutez et al., 2011). This is in line with reports linking LRRK2 function to Rho GTPases, which play a critical role in neurite growth by the remodeling of actin cytoskeleton (Chan et al., 2011; Habig et al., 2013) and also imbalances in the related Akt/PI3k pathway regulating survival in PD (Romani-Aumedes et al., 2014). For instance, miR-135a-5p has been shown to target the 3′-UTR and inhibit mRNA translation of Rho-associated protein kinase 2, which promotes neurodegeneration during the progression of PD in neuronal cells, acting as a compensatory mechanism (Liu et al., 2016; Saal et al., 2017). It is important to mention that the PD DAn cells studied here showed reduced axonal outgrowth and survival via caspase 3 cleavage, among other phenotypes, on the 75-days long-term culture (Sanchez-Danes et al., 2012b). Although we do not provide a functional link of these long-term functional alterations with early miRNA deregulation at 30-days culture, it could be plausible that these processes are related.

We also found that DEmiR identified in PD are associated with gene expression changes suggesting a role in regulating gene expression, which we observed can occur both inversely and positively. Focusing in classical direct inverse DEmiR/DEG associations, we found 2 miRNA/mRNA clusters including cluster 1 that encompassed PD downregulated DEmiRs and associated DEGs largely involved in specific neural functions, and cluster 2 comprising PD upregulated DEmiRs and associated DEGs overall related to diverse homeostatic functions. This finding adds a new layer of complexity to our PD DAn system providing additional molecular changes of miRNA expression correlating with previously observed gene expression changes (Fernandez-Santiago et al., 2015a). Our data also show that PD DEmiR alterations co-occur in early 30-days DAn cultures along with large PD-associated DNA methylation changes encompassing an hypermethylation of genomic enhancer elements, which is related to a deficit of a network of TF relevant to PD (*FOXA1*, *NR3C1*, *HNF4A*, and *FOSL2*) (Fernandez-Santiago et al., 2015a). More specifically, we found that upregulation of miR-9-5p and of miR-135b-5p were associated with

downregulation of *FOXA1* and *NR3C1*, respectively, suggesting a functional link between miRNA changes and gene expression levels of TF which are important for the correct epigenetic patterning of DAn in PD.

Our study has limitations. For instance, the sample size of 6 PD patients and 4 controls, although adequate for iPSC-based molecular studies, could still be considered somehow limited. In addition, the miRNA array used in the study screening 377 miRNAs, despite being genome-wide, does not analyze all described miRNAs and therefore additional miRNA could be investigated using our model. Finally, although we analyzed the functional relation between the identified PD-associated miRNA and gene expression alterations, we did not perform follow-up functional studies for the specific DEmiR detected. For these reasons, future studies using PD iPSC-derived DAn aimed at validating and expanding our findings are warranted.

Overall, miRNA profiles were largely similar in sPD and L2PD, which overall did not show differences in miRNA expression between each other. This finding is in line with previous transcriptomic, epigenomic (Fernandez-Santiago et al., 2015a), and phenotypic changes (Sanchez-Danes et al., 2012b) previously observed in PD DAn, which were also largely common in sPD and L2PD. Our results also agree with previous reports showing that, yet with specific differences (Marras et al., 2016), L2PD largely resembles common sPD clinically and neuropathologically (Healy et al., 2008). In addition, our study uncovers changes of miRNA expression, which are associated with PD and co-occur with transcriptomic and epigenomic changes antedating late PD neurodegenerative phenotypes. Altogether our findings suggest that multilayered molecular changes occur simultaneously in PD, a concept which is compatible with the well-accepted complex multifactorial character of disease. Moreover, our PD DAn model exhibited miRNA expression alterations that were previously reported in other biological samples from PD patients such as PD peripheral blood (miR-9-5p), serum (miR-141-3p), peripheral blood mononuclear cells (miR-199a-5p), SNpc (miR-135b-5p, miR-299–5p), putamen, and CSF (miR-9 and miR-449b). Finally, our study also indicates that iPSC-derived DAn from PD patients can prove a useful humanized cell system which, while preserving the patient genomic background, can recapitulate molecular alterations occurring in PD providing a unique tool to model disease at the cellular level.

## Disclosure statement

The authors report no actual or potential conflict of interest including any financial, personal, or other relationships with other people or organizations within 3 years of beginning the work submitted that could inappropriately influence this work.

## Acknowledgements

The authors thank the patients who participated in the study and their family members. The authors also thank Yvonne Richaud-Patin, Adriana Sánchez-Danés, Iria Carballo-Carbajal, and Miquel Vila, who contributed in the generation and characterization of the induced dopaminergic neurons from PD patients. This work was supported by funds from the Spanish Ministry of Economy and Competitiveness (MINECO) to R.F.-S. (grant # SAF2015-73508-JIN) (AEI/FEDER/UE), the Fondo de Investigaciones Sanitarias of the Instituto de Salud Carlos III (ISCIII) to M.E. (grant # PI14/00426), the Centro de Investigación Biomédica en Red de Enfermedades Neurodegenerativas (CIBERNED) to the Movement Disorders Unit of the Neurology Service from the Hospital Clínic de Barcelona to E.T., M.-J.M., R.F.-S., M.E., and C.G. (grant # PRI-16-2017). This work was also supported by BFU2013-49157-P, BFU2016-80870-P, and the European Research Council (ERC) 2012-StG (311736- PD-HUMMODEL) to A.C; ISCIII/FEDER (RD16/0011/0024) and Generalitat de Catalunya (2014-SGR-1460) to A.R.; and ISCIII/FEDER (PIE14/00061) to A.R. and M.-J.M. The authors also thank the CERCA Program from the Generalitat de Catalunya and the FEDER Program from the European Union to IDIBAPS and CMRB. Part of this work was developed at the Centre de Recerca Biomèdica Cellex (CRBC) from IDIBAPS/Hospital Clínic de Barcelona, Barcelona, Spain.

## Appendix A. Supplementary data

Supplementary data associated with this article can be found, in the online version, at https://doi.org/10.1016/j.neurobiolaging.2018.05.032.

## References

Abe, M., Bonini, N.M., 2013. MicroRNAs and neurodegeneration: role and impact. Trends Cell Biol. 23, 30–36.

Alieva, A., Filatova, E.V., Karabanov, A.V., Illarioshkin, S.N., Limborska, S.A., Shadrina, M.I., Slominsky, P.A., 2015. miRNA expression is highly sensitive to a drug therapy in Parkinson's disease. Parkinsonism Relat. Disord. 21, 72–74.

Anderegg, A., Lin, H.P., Chen, J.A., Caronia-Brown, G., Cherepanova, N., Yun, B., Joksimovic, M., Rock, J., Harfe, B.D., Johnson, R., Awatramani, R., 2013. An Lmx1b-miR135a2 regulatory circuit modulates Wnt1/Wnt signaling and determines the size of the midbrain dopaminergic progenitor pool. PLoS Genet. 9, e1003973.

Bartel, D.P., 2009. MicroRNAs: target recognition and regulatory functions. Cell 136, 215–233.

Benjamini, Y., Hochberg, Y., 1995. Controlling the false discovery rate: a practical and powerful approach to multiple testing. J. R. Stat. Soc. Series B Stat. Methodol. 57, 289–300.

Briggs, C.E., Wang, Y., Kong, B., Woo, T.U., Iyer, L.K., Sonntag, K.C., 2015. Midbrain dopamine neurons in Parkinson's disease exhibit a dysregulated miRNA and target-gene network. Brain Res. 1618, 111–121.

Botta-Orfila, T., Tolosa, E., Gelpi, E., Sanchez-Pla, A., Marti, M.J., Valldeoriola, F., Fernandez, M., Carmona, F., Ezquerra, M., 2012. Microarray expression analysis in idiopathic and LRRK2-associated Parkinson's disease. Neurobiol. Dis. 45, 462–468.

Cardo, L.F., Coto, E., Ribacoba, R., Menendez, M., Moris, G., Suarez, E., Alvarez, V., 2014. MiRNA profile in the substantia nigra of Parkinson's disease and healthy subjects. J. Mol. Neurosci. 54, 830–836.

Chan, D., Citro, A., Cordy, J.M., Shen, G.C., Wolozin, B., 2011. Rac1 protein rescues neurite retraction caused by G2019S leucine-rich repeat kinase 2 (LRRK2). J. Biol. Chem. 286, 16140–16149.

Chatterjee, P., Bhattacharyya, M., Bandyopadhyay, S., Roy, D., 2014. Studying the system-level involvement of microRNAs in Parkinson's disease. PLoS One 9, e93751.

Danborg, P.B., Simonsen, A.H., Waldemar, G., Heegaard, N.H., 2014. The potential of microRNAs as biofluid markers of neurodegenerative diseases–a systematic review. Biomarkers. 19, 259–268.

Dimmeler, S., Nicotera, P., 2013. MicroRNAs in age-related diseases. EMBO Mol. Med. 5, 180–190.

Dong, H., Wang, C., Lu, S., Yu, C., Huang, L., Feng, W., Xu, H., Chen, X., Zen, K., Yan, Q., Liu, W., Zhang, C., Zhang, C.Y., 2016. A panel of four decreased serum microRNAs as a novel biomarker for early Parkinson's disease. Biomarkers 21, 129–137.

Edwards, Y.J., Beecham, G.W., Scott, W.K., Khuri, S., Bademci, G., Tekin, D., Martin, E.R., Jiang, Z., Mash, D.C., ffrench-Mullen, J., Pericak-Vance, M.A., Tsinoremas, N., Vance, J.M., 2011. Identifying consensus disease pathways in Parkinson's disease using an integrative systems biology approach. PLoS One 6, e16917.

Fernandez-Santiago, R., Carballo-Carbajal, I., Castellano, G., Torrent, R., Richaud, Y., Sanchez-Danes, A., Vilarrasa-Blasi, R., Sanchez-Pla, A., Mosquera, J.L., Soriano, J., Lopez-Barneo, J., Canals, J.M., Alberch, J., Raya, A., Vila, M., Consiglio, A., Martin-Subero, J.I., Ezquerra, M., Tolosa, E., 2015a. Aberrant epigenome in iPSC-derived dopaminergic neurons from Parkinson's disease patients. EMBO Mol. Med. 7, 1529–1546.

Fernández-Santiago, R., Garrido, A., Infante, J., González-Aramburu, I., Sierra, M., Fernández, M., Valldeoriola, F., Muñoz, E., Compta, Y., Martí, M.J., Ríos, J., Tolosa, E., Ezquerra, M., 2015b. Barcelona LRRK2 Study Group, α-synuclein (SNCA) but not dynamin 3 (DNM3) influences age at onset of leucine-rich repeat kinase 2 (LRRK2) Parkinson's disease in Spain. Mov. Disord 33, 637–641.

Fernandez-Santiago, R., Iranzo, A., Gaig, C., Serradell, M., Fernandez, M., Tolosa, E., Santamaria, J., Ezquerra, M., 2015c. MicroRNA association with synucleinopathy conversion in rapid eye movement behavior disorder. Ann. Neurol. 77, 895–901.

Flor, I., Spiekermann, M., Loning, T., Dieckmann, K.P., Belge, G., Bullerdiek, J., 2016. Expression of microRNAs of C19MC in different histological types of testicular germ cell tumour. Cancer Genomics Proteomics 13, 281–289.

Fuchs, J., Mueller, J.C., Lichtner, P., Schulte, C., Munz, M., Berg, D., Wullner, U., Illig, T., Sharma, M., Gasser, T., 2009. The transcription factor PITX3 is associated with sporadic Parkinson's disease. Neurobiol. Aging 30, 731–738.
Gasser, T., 2009. Mendelian forms of Parkinson's disease. Biochim. Biophys. Acta 1792, 587–596.
Grunblatt, E., Mandel, S., Jacob-Hirsch, J., Zeligson, S., Amariglio, N., Rechavi, G., Li, J., Ravid, R., Roggendorf, W., Riederer, P., Youdim, M.B., 2004. Gene expression profiling of parkinsonian substantia nigra pars compacta; alterations in ubiquitin-proteasome, heat shock protein, iron and oxidative stress regulated proteins, cell adhesion/cellular matrix and vesicle trafficking genes. J. Neural Transm. (Vienna) 111, 1543–1573.
Habig, K., Gellhaar, S., Heim, B., Djuric, V., Giesert, F., Wurst, W., Walter, C., Hentrich, T., Riess, O., Bonin, M., 2013. LRRK2 guides the actin cytoskeleton at growth cones together with ARHGEF7 and Tropomyosin 4. Biochim. Biophys. Acta 1832, 2352–2367.
Healy, D.G., Falchi, M., O'Sullivan, S.S., Bonifati, V., Durr, A., Bressman, S., Brice, A., Aasly, J., Zabetian, C.P., Goldwurm, S., Ferreira, J.J., Tolosa, E., Kay, D.M., Klein, C., Williams, D.R., Marras, C., Lang, A.E., Wszolek, Z.K., Berciano, J., Schapira, A.H., Lynch, T., Bhatia, K.P., Gasser, T., Lees, A.J., Wood, N.W., International, L.C., 2008. Phenotype, genotype, and worldwide genetic penetrance of LRRK2-associated Parkinson's disease: a case-control study. Lancet Neurol. 7, 583–590.
Heman-Ackah, S.M., Hallegger, M., Rao, M.S., Wood, M.J., 2013. RISC in PD: the impact of microRNAs in Parkinson's disease cellular and molecular pathogenesis. Front Mol. Neurosci. 6, 40.
Hesse, M., Arenz, C., 2014. miRNAs as novel therapeutic targets and diagnostic biomarkers for Parkinson's disease: a patent evaluation of WO2014018650. Expert Opin. Ther. Pat. 24, 1271–1276.
Khoo, S.K., Petillo, D., Kang, U.J., Resau, J.H., Berryhill, B., Linder, J., Forsgren, L., Neuman, L.A., Tan, A.C., 2012. Plasma-based circulating MicroRNA biomarkers for Parkinson's disease. J. Parkinsons Dis. 2, 321–331.
Kim, J., Inoue, K., Ishii, J., Vanti, W.B., Voronov, S.V., Murchison, E., Hannon, G., Abeliovich, A., 2007. A MicroRNA feedback circuit in midbrain dopamine neurons. Science 317, 1220–1224.
Kumar, A., Kopra, J., Varendi, K., Porokuokka, L.L., Panhelainen, A., Kuure, S., Marshall, P., Karalija, N., Harma, M.A., Vilenius, C., Lillevali, K., Tekko, T., Mijatovic, J., Pulkkinen, N., Jakobson, M., Jakobson, M., Ola, R., Palm, E., Lindahl, M., Stromberg, I., Voikar, V., Piepponen, T.P., Saarma, M., Andressoo, J.O., 2015. GDNF overexpression from the native locus reveals its role in the nigrostriatal dopaminergic system function. PLoS Genet. 11, e1005710.
Lang, A.E., Lozano, A.M., 1998a. Parkinson's disease. First of two parts. N. Engl. J. Med. 339, 1044–1053.
Lang, A.E., Lozano, A.M., 1998b. Parkinson's disease. Second of two parts. N. Engl. J. Med. 339, 1130–1143.
Liu, C.G., Wang, J.L., Li, L., Xue, L.X., Zhang, Y.Q., Wang, P.C., 2014. MicroRNA-135a and -200b, potential Biomarkers for Alzheimers disease, regulate beta secretase and amyloid precursor protein. Brain Res. 1583, 55–64.
Liu, Y., Liao, S., Quan, H., Lin, Y., Li, J., Yang, Q., 2016. Involvement of microRNA-135a-5p in the protective effects of hydrogen sulfide against Parkinson's disease. Cell Physiol. Biochem. 40, 18–26.
Mandel, S., Grunblatt, E., Riederer, P., Amariglio, N., Jacob-Hirsch, J., Rechavi, G., Youdim, M.B., 2005. Gene expression profiling of sporadic Parkinson's disease substantia nigra pars compacta reveals impairment of ubiquitin-proteasome subunits, SKP1A, aldehyde dehydrogenase, and chaperone HSC-70. Ann. N Y Acad. Sci. 1053, 356–375.
Margis, R., Margis, R., Rieder, C.R., 2011. Identification of blood microRNAs associated to Parkinsonis disease. J. Biotechnol. 152, 96–101.
Marras, C., Alcalay, R.N., Caspell-Garcia, C., Coffey, C., Chan, P., Duda, J.E., Facheris, M.F., Fernandez-Santiago, R., Ruiz-Martinez, J., Mestre, T., Saunders-Pullman, R., Pont-Sunyer, C., Tolosa, E., Waro, B. LRRK2 Cohort Consortium, 2016. Motor and nonmotor heterogeneity of LRRK2-related and idiopathic Parkinson's disease. Mov. Disord. 31, 1192–1202.
Martins, M., Rosa, A., Guedes, L.C., Fonseca, B.V., Gotovac, K., Violante, S., Mestre, T., Coelho, M., Rosa, M.M., Martin, E.R., Vance, J.M., Outeiro, T.F., Wang, L., Borovecki, F., Ferreira, J.J., Oliveira, S.A., 2011. Convergence of miRNA expression profiling, alpha-synuclein interacton and GWAS in Parkinson's disease. PLoS One 6, e25443.
Mutez, E., Larvor, L., Lepretre, F., Mouroux, V., Hamalek, D., Kerckaert, J.P., Perez-Tur, J., Waucquier, N., Vanbesien-Mailliot, C., Duflot, A., Devos, D., Defebvre, L., Kreisler, A., Frigard, B., Destee, A., Chartier-Harlin, M.C., 2011. Transcriptional profile of Parkinson blood mononuclear cells with LRRK2 mutation. Neurobiol. Aging 32, 1839–1848.
Reeve, A., Simcox, E., Turnbull, D., 2014. Ageing and Parkinson's disease: why is advancing age the biggest risk factor? Ageing Res. Rev. 14, 19–30.
Ritchie, W., Rajasekhar, M., Flamant, S., Rasko, J.E., 2009. Conserved expression patterns predict microRNA targets. PLoS Comput. Biol. 5, e1000513.
Romani-Aumedes, J., Canal, M., Martin-Flores, N., Sun, X., Perez-Fernandez, V., Wewering, S., Fernandez-Santiago, R., Ezquerra, M., Pont-Sunyer, C., Lafuente, A., Alberch, J., Luebbert, H., Tolosa, E., Levy, O.A., Greene, L.A., Malagelada, C., 2014. Parkin loss of function contributes to RTP801 elevation and neurodegeneration in Parkinson's disease. Cell Death Dis. 5, e1364.
Saal, K.A., Galter, D., Roeber, S., Bahr, M., Tonges, L., Lingor, P., 2017. Altered expression of growth associated Protein-43 and Rho kinase in human patients with Parkinson's disease. Brain Pathol. 27, 13–25.
Sales, G., Coppe, A., Bisognin, A., Biasiolo, M., Bortoluzzi, S., Romualdi, C., 2010. MAGIA, a web-based tool for miRNA and genes integrated analysis. Nucleic Acids Res. 38, W352–W359.
Sanchez-Danes, A., Consiglio, A., Richaud, Y., Rodriguez-Piza, I., Dehay, B., Edel, M., Bove, J., Memo, M., Vila, M., Raya, A., Izpisua Belmonte, J.C., 2012a. Efficient generation of A9 midbrain dopaminergic neurons by lentiviral delivery of LMX1A in human embryonic stem cells and induced pluripotent stem cells. Hum. Gene Ther. 23, 56–69.
Sanchez-Danes, A., Richaud-Patin, Y., Carballo-Carbajal, I., Jimenez-Delgado, S., Caig, C., Mora, S., Di Guglielmo, C., Ezquerra, M., Patel, B., Giralt, A., Canals, J.M., Memo, M., Alberch, J., Lopez-Barneo, J., Vila, M., Cuervo, A.M., Tolosa, E., Consiglio, A., Raya, A., 2012b. Disease-specific phenotypes in dopamine neurons from human iPS-based models of genetic and sporadic Parkinson's disease. EMBO Mol. Med. 4, 380–395.
Serafin, A., Foco, L., Zanigni, S., Blankenburg, H., Picard, A., Zanon, A., Giannini, G., Pichler, I., Facheris, M.F., Cortelli, P., Pramstaller, P.P., Hicks, A.A., Domingues, F.S., Schwienbacher, C., 2015. Overexpression of blood microRNAs 103a, 30b, and 29a in L-dopa-treated patients with PD. Neurology 84, 645–653.
Shannon, P., Markiel, A., Ozier, O., Baliga, N.S., Wang, J.T., Ramage, D., Amin, N., Schwikowski, B., Ideker, T., 2003. Cytoscape: a software environment for integrated models of biomolecular interaction networks. Genome Res. 13, 2498–2504.
Soreq, L., Salomonis, N., Bronstein, M., Greenberg, D.S., Israel, Z., Bergman, H., Soreq, H., 2013. Small RNA sequencing-microarray analyses in Parkinson leukocytes reveal deep brain stimulation-induced splicing changes that classify brain region transcriptomes. Front Mol. Neurosci. 6, 10.
Vallelunga, A., Ragusa, M., Di Mauro, S., Iannitti, T., Pilleri, M., Biundo, R., Weis, L., Di Pietro, C., De Iuliis, A., Nicoletti, A., Zappia, M., Purrello, M., Antonini, A., 2014. Identification of circulating microRNAs for the differential diagnosis of Parkinson's disease and Multiple System Atrophy. Front Cell Neurosci. 8, 156.
Vandesompele, J., De Preter, K., Pattyn, F., Poppe, B., Van Roy, N., De Paepe, A., Speleman, F., 2002. Accurate normalization of real-time quantitative RT-PCR data by geometric averaging of multiple internal control genes. Genome Biol. 3. RESEARCH0034.
Vlachos, I.S., Paraskevopoulou, M.D., Karagkouni, D., Georgakilas, G., Vergoulis, T., Kanellos, I., Anastasopoulos, I.L., Maniou, S., Karathanou, K., Kalfakakou, D., Fevgas, A., Dalamagas, T., Hatzigeorgiou, A.G., 2015a. DIANA-TarBase v7.0: indexing more than half a million experimentally supported miRNA:mRNA interactions. Nucleic Acids Res. 43, D153–D159.
Vlachos, I.S., Zagganas, K., Paraskevopoulou, M.D., Georgakilas, G., Karagkouni, D., Vergoulis, T., Dalamagas, T., Hatzigeorgiou, A.G., 2015b. DIANA-miRPath v3.0: deciphering microRNA function with experimental support. Nucleic Acids Res. 43, W460–W466.
Wei, Y., He, R., Wu, Y., Gan, B., Wu, P., Qiu, X., Lan, A., Chen, G., Wang, Q., Lin, X., Chen, Y., Mo, Z., 2016. Comprehensive investigation of aberrant microRNA profiling in bladder cancer tissues. Tumour Biol. 37, 12555–12569.
Wu, J., Bao, J., Kim, M., Yuan, S., Tang, C., Zheng, H., Mastick, G.S., Xu, C., Yan, W., 2014. Two miRNA clusters, miR-34b/c and miR-449, are essential for normal brain development, motile ciliogenesis, and spermatogenesis. Proc. Natl. Acad. Sci. U. S. A. 111, E2851–E2857.